

SMASIS2016-9292

**FIRST STEPS IN MODELING THERMAL ACTUATION OF TWISTED POLYMER
ACTUATORS USING VIRGIN MATERIAL PROPERTIES**

Michael W. Shafer

Assistant Professor
Dept. of Mechanical Engineering
Northern Arizona University
Flagstaff, Arizona 86001
Email: Michael.Shafer@nau.edu

Heidi P. Feigenbaum

Associate Professor
Dept. of Mechanical Engineering
Northern Arizona University
Flagstaff, Arizona 86001
Email: Heidi.Feigenbaum@nau.edu

Daniel Pugh

Undergraduate Student
Dept. of Mechanical Engineering
Northern Arizona University
Flagstaff, Arizona 86001

Matthew Fisher

Undergraduate Student
Dept. of Mechanical Engineering
Northern Arizona University
Flagstaff, Arizona 86001

ABSTRACT

Artificial muscle systems have the potential to impact many technologies ranging from advanced prosthesis to miniature robotics. Recently, it has been shown that twisting drawn polymer fibers such as nylon can result in torsional or tensile actuators depending on the final fiber configuration. The actuation phenomenon relies on the anisotropic nature of the fibers moduli and thermal expansion. They have high axial stiffness, low shear stiffness, and expand more radially when heated than axially. If a polymer fiber is twisted but not coiled, these characteristics result in a torsional actuator that will untwist when heated. During the fabrication process, these twisted polymers can be configured helically before annealing. In this configuration, the untwisting that occurs in a straight twisted fiber results in a contraction or extension depending on relative directions of twist and coiling. In these ways, these materials can be used to create both torsional or axial actuators with extremely high specific work capabilities. To date, the focus of research on twisted polymer actuators (TPAs) and twisted-coiled polymer actuators (TCPAs) has been actuator characterization that demonstrates the technologies

capabilities. Our work focuses here on applying a 2D analysis of individual layers of the TPAs to predict thermally induced twisting angle and fiber length based on virgin (untwisted) material properties and actuator parameters like fiber length and inserted twist. A multi-axis rheometer with a controlled thermal environmental chamber was used to twist, anneal, and test thermally induced actuation. Experimentally measured angle of untwist and axial contraction after heating are compared to the model. In comparing the experimental results with the two dimensional model, it appears that the difference between the 2D model and experimental results can be explained by the longitudinal stresses that develop inside the material. Future work will aim to include these effects in the model in order to be able to use this model in the design of TPAs.

1 Introduction

A variety of technologies and materials have been proposed as artificial muscles. Shape-memory alloys (SMA) are a type of “smart-material” that can return to a preset shape after some mechanical deformation and thereby act as an actuator. Spun car-

bon nanotube (CNT) yarns have also been employed as synthetic muscles [1, 2]. The expense of SMAs and CNT yarns impede wide scale deployments of the technologies. Conversely, it was recently discovered that extremely inexpensive drawn polymer monofilaments, such as nylon and polyethylene that are used in fishing line, have anisotropic thermal expansion characteristics and can actuate similarly to CNT yarns. By twisting and coiling the fishing line, extremely powerful, lightweight, and inexpensive thermally-activated actuators can be made whose specific load capacity is higher than human muscle [3].

In discussing these actuators, it is important to understand the differences in terminology regarding twist and coiling. A precursor fiber is considered to be a straight drawn polymer fiber, while a twisted fiber is one in which a precursor fiber is twisted about its central axis but remains straight. Although a twisted fiber will remain straight, after twisting its polymer chains will then be helically oriented about the fiber axis with a pitch angle that depends in radial position (see Fig. 1). Typically, after twisting the material is annealed so that internal stresses are relieved and the material remains twisted when unloaded. Coiling refers to a fiber, twisted or untwisted, that is annealed in a helical configuration. This helical configuration can be developed by increasing the amount of twist in a precursor fiber to a point at which the fiber torsionally buckles and coils over on itself. Alternatively, a twisted or untwisted fiber can be wrapped around a mandrel prior to annealing. Depending on the final configuration of the polymer fiber, a variety of combinations are possible, but the most typical would be twisted-coiled polymer actuators (TCPAs) which provide linear actuation and twisted polymer actuators (TPAs) which provide torsional actuation.

To date, research on TPAs and TCPAs has focused on experimentally exploring the actuation phenomenon and characterizing actuator performance [3–6]. Due in part to the novelty of these devices, the complex geometry of the coiling, and the experimental challenges in model validation, there is limited work on the analytic modeling of these synthetic actuators. Because of their simpler geometry, the modeling work to date has focused on TPAs rather than TCPAs. Aziz et al. [7] used the thermal expansion properties of twisted fibers along with classical torsion theory to model TPAs and got good agreement with experimental results for both torsional stroke, i.e. untwist, and blocked torque, i.e. torque that develops when the heated fibers are securely clamped. However, using thermal expansion of the twisted fibers for design purposes can be limiting because it requires experimental tests whenever a new initial twist is inserted. Additionally, their work assumed no length changes in the twisted fibers. Ideally, the relationship between torque or force, displacement, and temperature would be modeled based on precursor fiber material properties; thereby drastically decreasing the materials testing requirements and allowing for the design of the initial twist based on desired performance of the actuator.

In this work, we present a preliminary model for the re-

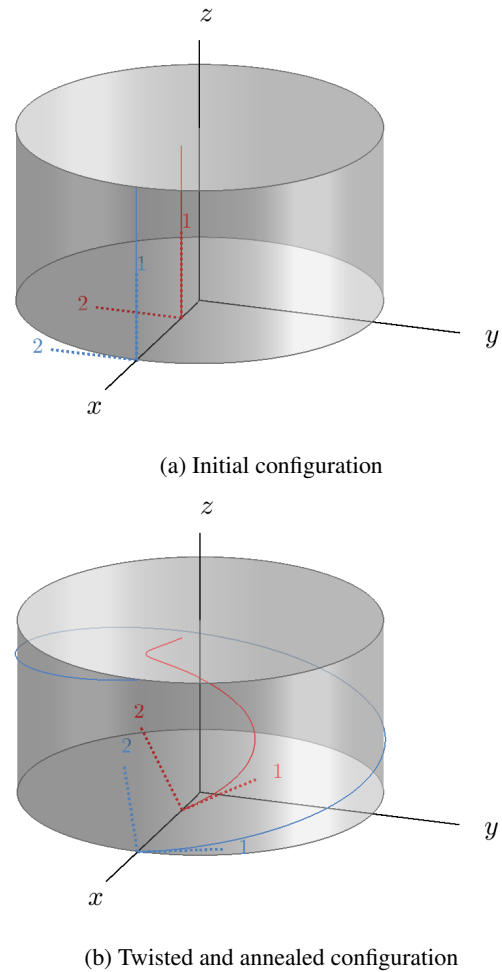


FIGURE 1: Conceptual diagram showing (a) untwisted and (b) twisted monofilament with lines representing polymer chain configurations. Notices that angle of polymer chain (1-direction) with respect to the $x - y$ plane (α) depends on radial position after twisting.

sponse of twisted polymer actuators (TPAs) subject to thermal load. We focus here on a structural model that relates the geometrical configuration to the response to thermal loading. Our experimentation uses a nylon 6 monofilament, but the focus of this work is not on modeling the material itself, for that we assume linear elastic orthotropic material behavior, but rather on modeling the twisted structure. Towards this end, we assume that the material properties reorient (change direction) when the material is twisted and annealed, but do not change magnitude. Thus, the model in this work only uses material properties that can be identified on the untwisted polymer monofilaments and actuator properties like the initial length and inserted twist to predict the behavior of TPAs. This model is 2D and essentially considers

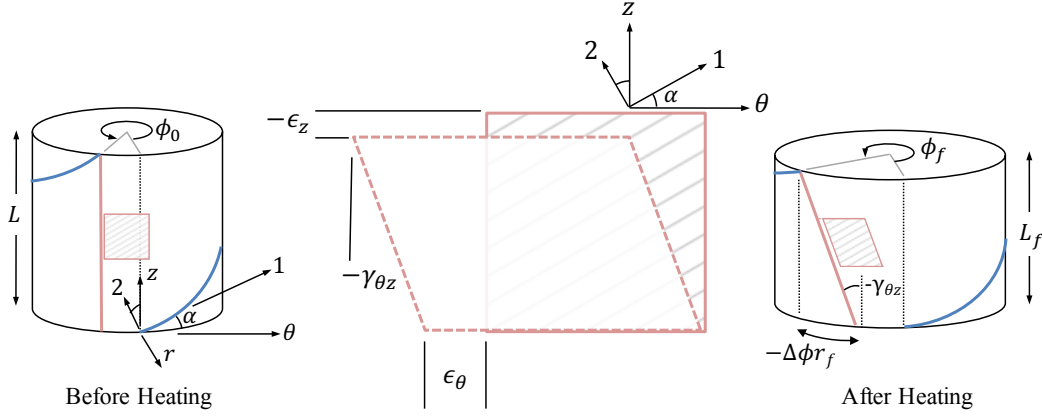


FIGURE 2: Sections of TPA before and after heating with elemental 2D section shown on both, as well as enlarged between the two. The elemental section shows shear, axial, and tangential strains resulting from thermal loading of a twisted polymer. Radial (r), tangential (θ) and axial (z) coordinates, as well as the polymer chain coordinates (1 & 2 directions) are shown. Notice that 1 and 2 directions are rotated from θ and z directions by angle α . This rotation is due to the initial twist angle shown as ϕ_0 , which is maintained due to annealing. The initial angle ϕ_0 is changed to ϕ_f after heating as a result of a thermally induced twisting by angle $-\Delta\phi$.

each radial position as an independent element. We focus here on capturing the temperature-displacement phenomenon, with plans to include torque generation in the future. As part of this modeling effort, we show that the general method of transformation of material properties is able to capture the major effects of the temperature-displacement relationship. We also show that the length changes of the TPA that are often neglected in other works, while small in magnitude, impose a radially varying axial stress that likely contributes to the untwisting actuation performance. When this model is compared to experimental results, it can be seen that the difference in the experimental results qualitatively conform to the differences that would be expected if the three dimensional effects were included. Additionally, here we present a novel method of fabrication and testing of TPAs using a rheometer.

2 Modeling TPAs subject to Thermal Loads

The model proposed here is based on the assumption that the polymer actuators can be treated as a bundle of polymer chains and thus an anisotropic linear-elastic material. Additionally, we assume that material properties, such as the elastic modulus and thermal expansion functions, in the directions perpendicular to the polymer chain direction are different than in the polymer chain direction. Two of these polymer chains are shown conceptually in Fig. 1 for a twisted fiber. Notice that the individual chains are at different radial positions, and therefore are at different pitch angles, α , measured from the horizontal after being twisted and annealed. The pitch angle of each chain depends on the distance from the center of the monofilament and the amount of inserted twist. A chain at the center will not be twisted at all

($\alpha = 90^\circ$), whereas chains on the outermost edge of the monofilament will have lowest pitch angle off horizontal (α will be smallest). Typically, these outer polymer chain angles are on the order of 30-60°.

Conceptual 1D descriptions of the actuation phenomenon for TPAs consistently rely on the “unwrapping” of one of these polymer chains from the outer most radial position. This method of describing the actuation is sufficient for demonstrating the overall untwisting phenomenon, but is insufficient when attempting to model how thermal expansion response in the different material directions quantitatively affects the angle of untwist. When modeling these actuators based on precursor fiber material properties, the radial, tangential, and longitudinal direction material properties need to be properly transformed, which cannot be accomplished using a 1D element. Others have found good agreement using a 1D modeling method, but while using material properties from twisted and annealed samples wherein the measurement of the material properties already included this transformation.

If we unwrap a section of a cylindrical layer from any given radial position, the result is essentially a 2D element with material properties that are the same as the original fiber properties, but rotated by the pitch angle α (see Fig. 2). Because of this, the model will give different predictions for how the material responds to changes in response to thermal loading at different radii. This preliminary model does not include interactions between the layers at different radii, and instead this model assumes that the fibers at each radii are free to expand/contract due to thermal loading and are under no stress.

The model aims to use the virgin or untwisted axial (1-direction in Fig. 1a) thermal expansion function, ϵ'_{11} , and the

tangential (2-direction in Fig. 1a) thermal expansion, ϵ'_{22} to predict the untwist ($\Delta\phi$) and change in length ($L_f - L$) of the polymer monofilament under thermal loading as shown in Fig. 2. Assuming that ϵ'_{11} and ϵ'_{22} are known, and that thermal loads causes no shear deformation of the untwisted fibers ($\gamma'_{12} = 0$), the thermal strains of the twisted fibers can be found using a classic coordinate transformation:

$$\begin{Bmatrix} \epsilon'_\theta \\ \epsilon'_z \\ \frac{1}{2}\gamma'_{z\theta} \end{Bmatrix} = \begin{bmatrix} \cos^2 \alpha & \sin^2 \alpha & -2 \cos \alpha \sin \alpha \\ \sin^2 \alpha & \cos^2 \alpha & 2 \cos \alpha \sin \alpha \\ \cos \alpha \sin \alpha & -\cos \alpha \sin \alpha & \cos^2 \alpha - \sin^2 \alpha \end{bmatrix} \begin{Bmatrix} \epsilon'_{11} \\ \epsilon'_{22} \\ 0 \end{Bmatrix} \quad (1)$$

These strains are illustrated conceptually in Fig. 2.

The thermal strain of the monofilament, ϵ'_θ , ϵ'_z , and $\gamma'_{z\theta}$ can be simplified by defining a non-dimensional initial twist $x = \frac{r\phi_0}{L}$, where r is the radius at the location of a particular fiber, ϕ_0 is the initial twist put into the fibers, and L is the initial length of the monofilament (see figure 2) that varies between 0 and a maximum of $\frac{R\phi_0}{L}$, where R is the monofilament radius. With this non-dimensional parameter, it can be shown that

$$\cos^2 \alpha = \frac{x^2}{1+x^2} \quad (2)$$

$$\sin^2 \alpha = \frac{1}{1+x^2} \quad (3)$$

and therefore,

$$\epsilon'_\theta = \frac{\epsilon'_{11}x^2 + \epsilon'_{22}}{1+x^2} \quad (4)$$

$$\epsilon'_z = \frac{\epsilon'_{22}x^2 + \epsilon'_{11}}{1+x^2} \quad (5)$$

$$\gamma'_{z\theta} = 2(\epsilon'_{11} - \epsilon'_{22}) \frac{x}{1+x^2} \quad (6)$$

Notice that in the limit of symmetric thermal expansion, $\epsilon'_{11} = \epsilon'_{22}$, there would be no untwist of the fibers, $\gamma'_{z\theta} = 0$. Also notice that in the limit of no initial twist, $\phi_0 = 0$, which implies that $x = 0$, there would be no resulting shear deformation and thus no untwist of the fibers.

From ϵ'_z the change in length can be calculated as

$$\Delta L = L_f - L = \epsilon'_z L = \frac{\epsilon'_{22}x^2 + \epsilon'_{11}}{1+x^2} L \quad (7)$$

Since ϵ'_z depends on x , the change in length is different at various radii. Assuming that ϵ'_{11} is negative, i.e. in the fiber direction thermal contraction occurs, the inner most fiber would like to

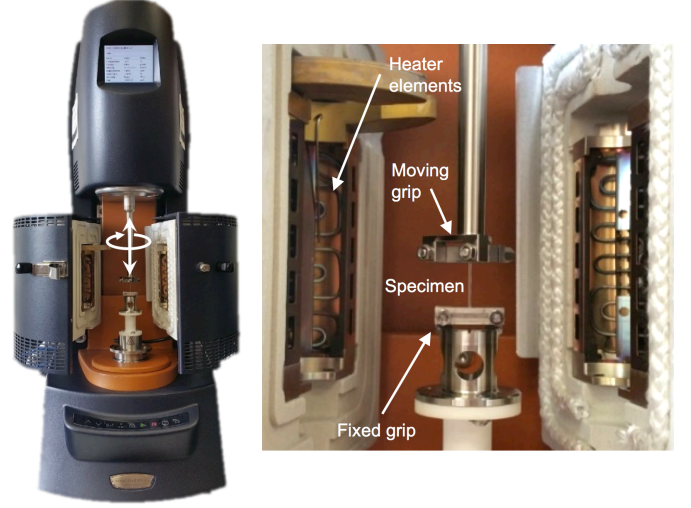


FIGURE 3: View of TA Instruments Hybrid Discover Rheometer 2 (HR-2) with an Environmental Test Chamber (ETC) and specimen within instrument. ETC open to show sample location and size.

contract the most, while the outermost fibers would like to contract the least, or expand the most.

As shown in Fig. 2, the untwist of the fibers is related to $\gamma'_{z\theta}$ via

$$\frac{\Delta\phi r}{L} = \tan \gamma'_{z\theta} \approx \gamma'_{z\theta} \quad (8)$$

This equation matches that from classical torsion theory. Solving for $\Delta\phi$ in Eq. (8), gives a prediction of untwist as follows:

$$\frac{\Delta\phi}{\phi_0} = \frac{(\epsilon'_{11} - \epsilon'_{22})}{1+x^2} \quad (9)$$

where ϵ'_{11} and ϵ'_{22} are given in section 3.1.

Note that in Eq. (8), small strains are assumed. We initially used $x = \frac{r_f\phi_f}{L_f}$, where $r_f = r(1 + \epsilon'_\theta)$, and $L_f = L(1 + \epsilon'_z)$ instead of x and L in Eq. (7) and Eq. (9). Additionally, we kept the tangent function in Eq. (8). We found these refinements to make the resulting expression much more complicated, resulting in an equation that required a numerical solution. These complications provided very little difference in the predicted results for $\Delta\phi$ and ΔL for the material and initial twists studied in this work.

3 Experimental methods

The material selected for experimental testing here was Berkley Trilene[®] Big Game[™] 80lb monofilament (nylon 6),

similar to the monofilament used by Haines et al. [3] but with a higher breaking strength. The diameter of the precursor fibers was 0.89 mm. Most of the experimental tests in this work were conducted on a TA Instruments Hybrid Discover Rheometer 2 (HR-2) with an Environmental Test Chamber (ETC) accessory attachment. Rheometer systems are typically employed to characterize viscous and viscoelastic materials, but the ability of the instrument to provide highly resolved force and torque measurements while maintaining and sweeping loads and displacements make it ideally suited for characterizing precursor, twisted, and coiled monofilaments. Moreover, this particular system allows for the fabrication (twisting and annealing) and testing of the fibers by the same device without ever removing the actuator from the rheometer. The result is extremely repeatable and consistent samples and experimental results.

The HR-2 system has the following measurement resolutions: Torque 0.1 nN-m; Force: 0.5 mN; Rotation: 10 nrad; Axial; 0.1 μm . The ETC attachment allows these test to be conducted at a regulated thermal environment, or while the temperature is swept. An image of a precursor fiber in the DH-2 system can be seen in figure 3 and shows the open ETC accessory. In this figure, a polymer fiber is shown clamped between two grips. The upper grip is attached to the moving head of the rheometer. The software that controls and runs experiments on this device allows for a large number experiments and allows these tests to be stitched together for sequential execution. For example, during fabrication of twisted samples, the rheometer maintains a specified axial tension, while rotating the head at a given rate. Upon completion, the system conducts a temperature ramp “test” that acts as the thermal annealing step.

3.1 Identification of Material Properties

The fundamental mechanism of actuation for these twisted and coiled monofilament is a result of the anisotropic nature of the thermal expansion of the material. As such, in order to predict the actuation of the material it is critical to accurately capture the thermal expansion of the virgin material, namely ϵ'_{11} and ϵ'_{22} . As previously mentioned, the radial and tangential thermal expansion would be equivalent, and thus we use radial thermal expansion results to determine 2-direction thermal expansion as shown in Fig. 1. We first characterized the axial dependence on temperature.

Axial expansion as a function of temperature was measured on the rheometer. A sample of straight untwisted precursor fiber, 27mm in length, was placed in the rheometer clamps with a gap of 15mm between the clamps. Prior to placement in the rheometer, the precursor fibers were put under light tension and annealed in an oven for 20 minutes at 126.6°C so that the fibers would remain straight. The following thermal expansion test procedure was done manually, however there are means of doing such a test automatically on this machine via the controller software.

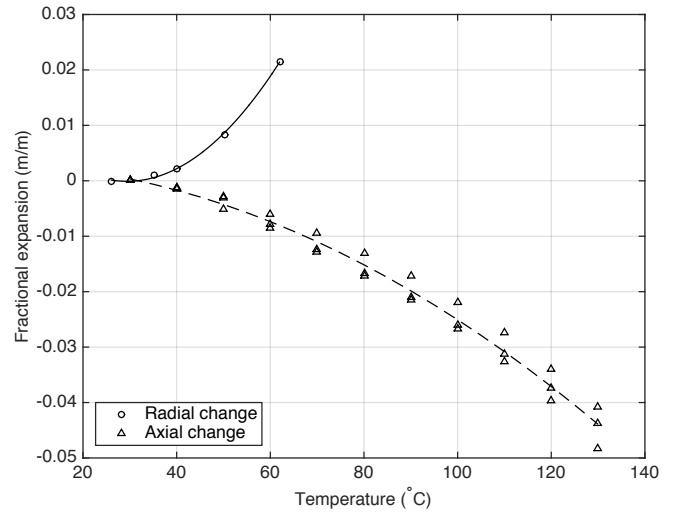


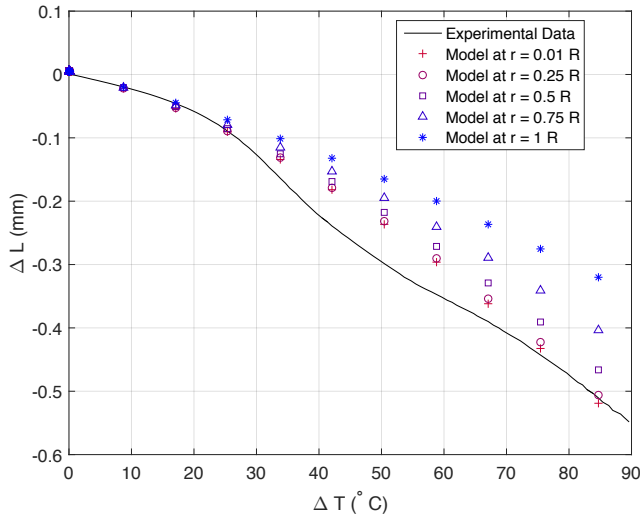
FIGURE 4: Radial and axial thermal expansion for precursor fibers. Radial data taken from Aziz et al. Fig. 4c for 0.78 mm diameter nylon 6 monofilament samples with close to vertical polymer chain angle of $\alpha = 70.4^\circ$ [7].

The rheometer was set to maintain a tensile load of 0 ± 0.1 N on the fiber. The tensile force controller on the rheometer has a resolution of 0.1 N, so this setting was applied in order to maintain a nearly zero load on the sample during heating. The ETC was then used to bring the sample up to temperatures ranging from 30°C to 130°C in 10°C increments. After reaching steady state at each temperature the sample length was recorded from the rheometer digital read out.

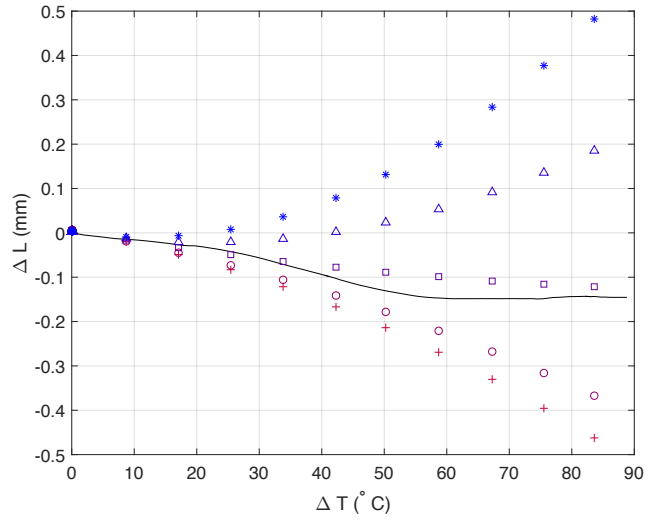
The results of three trials of this axial thermal expansion test can be seen in Fig. 4. The fractional change in fiber length (ϵ'_{11}) is shown as a function of temperature T . The results show a nonlinear thermal contraction over the temperature range. The second order polynomial fit shown in Fig. 4 is given by

$$\epsilon'_{11} = -2.657 \times 10^{-6} T^2 - 1.742 \times 10^{-5} T + 3.249 \times 10^{-3} \quad (10)$$

Radial thermal expansion for a drawn polymer fiber is challenging to measure directly. The small diameter and reduced modulus in the radial direction when heated make direct measurements via a micrometer or other instrument inaccurate. Indirect methods, such as measuring displaced fluid, are more involved but yield better results. Our initial efforts to measure radial thermal expansion involved measuring the displacement of a water-glycol mixture by the monofilament during heating. Although these tests were conducted relatively quickly, we saw evidence of the liquid mixture being absorbed by the monofilament. The samples took on the hue of the glycol mixture and the radial expansion results, while matching at low temperatures,



(a) $\phi_0 = 10$ rad



(b) $\phi_0 = 26.38$ rad

FIGURE 5: Experimental results and model predictions at various radii (where R is the total radius of the monofilament) of change in length of the monofilament due to thermal loading of a TPA with initial inserted twist of (a) $\phi_0 = 10$ radians and (b) $\phi_0 = 26.38$ radians. Legend in (a) also applies to (b).

deviated from published results at temperatures above approximately 50°C . In theory accounting for water absorption could be accomplished, but would required detailed measurements of swelling in both the radial and axial direction, adding another source of error and once again introducing the need to directly measure radius at temperature. While the inclusion of water absorption should be measured for some applications, especially since many TPAs and TCPAs are thermally cycled using flowing water, our axial expansion and untwisting experiments occurred in an air environment. We therefore required radial thermal expansion functions where water absorption was not included.

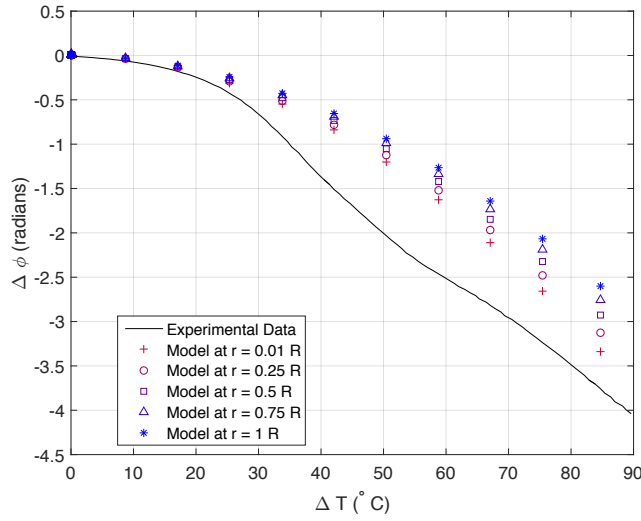
Aziz et al. measured radial thermal expansion using a similar fluid displacement method, but used a silicone oil as the working fluid [7]. Although their study was for twisted fibers, they reported the thermal expansion for an only slightly twisted fiber with an α angle of 70.4° for the outermost radial position. Recall that α for an untwisted precursor fiber would be 90° . They tested a range of material diameters with extremely repeatable radial thermal expansion results regardless of diameter. Based on these results, it is reasonable to assume that an untwisted nylon 6 monofilament would show the similar results for radial thermal expansion. The data from the work of Aziz et al. is presented in Fig. 4 along with the axial data we collected for our untwisted fibers. Like the axial results, a second order polynomial was fitted to the data. The 2-direction thermal expansion function is

thus

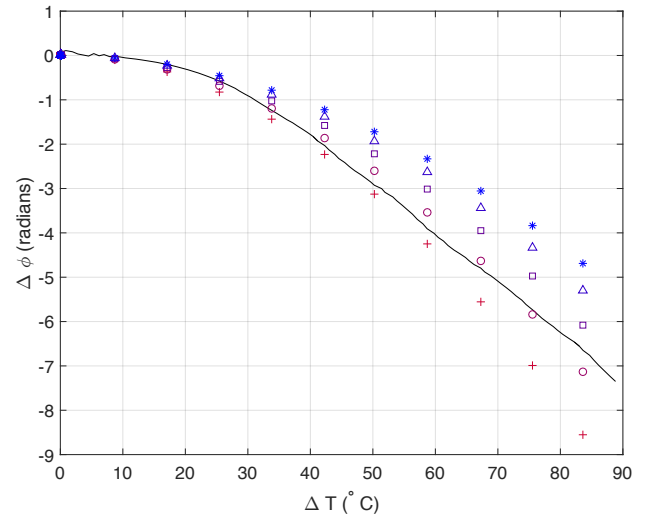
$$\epsilon_{22}^t = 2.023 \times 10^{-5} T^2 - 1.189 \times 10^{-3} T + 17.39 \times 10^{-3} \quad (11)$$

3.2 Fabrication of TPAs

In order to produce consistent TPAs with various amounts of twist, the rheometer was used to fabricate the samples. The straightened precursor fibers were placed in the rheometer clamps and tightened with a gap of 15mm between both clamps. Precursor fibers were centered in the rheometer clamps such that they aligned with the axis of the instrument's rotation. Next, a 15 ± 0.1 N axial load was applied to the sample through the rheometer. This load was selected based on trial and error and previous experience. The nylon was then twisted by setting the motor velocity on the rheometer to 0.1 rads/sec. This velocity was adequate to ensure that the rheometer could adjust the gap between the two grips fast enough to maintain an applied load close to the desired value. Once the nylon fiber reached an angular displacement close to that of the desired value, the velocity was set to 0 rads/sec. The sample was then rotationally locked by the instrument. Finally, the TPAs were annealed by setting the ETC temperature to 126.6°C . This temperature was found to work well for annealing base on previous laboratory trials. Samples were held at this temperature for 20 minutes while kept under a 15 ± 0.1 N axial force. The samples were then left to cool back to room temperature while kept under the 15 N axial force.



(a) $\phi_0 = 10$ rad



(b) $\phi_0 = 26.38$ rad

FIGURE 6: Experimental results and model predictions at various radii (where R is the total radius of the monofilament) of thermally actuated twist ($\Delta\phi$) of the monofilament of a TPA with initial inserted twist of (a) $\phi_0 = 10$ radians and (b) $\phi_0 = 26.38$ radians. Legend in (a) also applies to (b).

3.3 Thermal Loading and Untwisting of TPAs

In order to compare the 2D approximate model for untwist of TPAs based on thermal loading, an experimental procedure was developed using the rheometer. To match the loading conditions considered in the model, the samples placed in the rheometer would have nearly zero tensile and torsional load applied while heating and measuring displacement. Two different initial twists were tested ($\phi_0 = 10$ rad and $\phi_0 = 26.38$ rad) in order to investigate effects of initial twist angle and thus polymer chain angle on deformation. A temperature ramp from 30°C to 120°C at a rate of $5^\circ\text{C}/\text{min}$ was used. During these tests the torque was set to zero, while the axial force applied to the sample was 0.2 ± 0.1 N in tension. This small axial load was required to prevent experimental errors associated with the force resolution of the controller. We found if the axial force was set to zero, the relatively large resolution in the feedback controller for axial force would occasionally result in compressive forces into the fibers, which made accurate fiber length measurements impossible. The temperature ramp rate used allowed for the axial force to be maintained within the desired range. During the heating of the samples, the rheometer recorded gap length between sample grips, grip angle, and temperature.

4 Results and Discussion

Experimental results and model predictions for change in length of the monofilament and changes in twist are shown in Figs. 5a and 5b and 6a and 6b, respectively. In these figures,

model predictions are shown at radii ranging from $r = 1\%R$ – $100\%R$, where R is the total radius of the monofilament. Results are not shown at $r = 0$ because the model is 2D in nature, and $r = 0$ is a 1D line element, and therefore the model does not apply. As r approaches 0, $\gamma'_{z\theta}$ goes to 0 according to Eq. (6) and ΔL approaches ϵ'_{11} according to Eq. (7). But as Eqs. (8) and (9) show, $\Delta\phi$ converges to $(\epsilon'_{11} - \epsilon'_{22})\phi_0$ as r goes to 0, implying that untwist is needed to cause even a very small shear strain near the center of the monofilament.

Notice that the model predicts different changes in length at different radii. Near the center of the monofilament, the model predicts that the material wants to contract, according to Eq. (10), because fibers are aligned with the longitudinal (z) direction. At the outermost radii, the model predicts that the fibers want to contract significantly less or expand, depending on the temperature and initial twist inserted, due to the component of radial (2-direction) expansion now in the longitudinal (z) direction from the initial twist of the fibers. With the larger initial twist of $\phi_0 = 26.38$ rad in Fig. 5b there is significantly more spread between the model predictions at different radii than with the small initial twist of $\phi_0 = 10$ rad in Fig. 5a. This is expected, as with more twist there is more 2-direction component of the fibers in the longitudinal direction. This can also be seen from Eq. (7) where more twist implies the maximum values of x increases while the minimum remains 0, and thus ΔL also has more spread.

In both Figs. 5a and 5b the model at the smaller radii, 0.01 – $0.5R$, predicts the experimental results the best. The model con-

siders that fibers at each radii are free to expand/contract, but this is not strictly true. The monofilament must expand/contract as a single unit, and the results indicate that the fibers closer to the center or middle of the monofilament govern the change in length.

Moreover, fibers at different radii that want to axially expand or contract differently will cause stresses between the radial layers that are not captured by the current 2D model. We think that these internal stresses and the fact that the overall length change of the monofilament follows that of the inner or middle fibers can explain the predictions of untwist in Figs. 6a and 6b. In general, the outer fibers want to contract less or expand more than the TPA as a whole does. Therefore we would expect a longitudinal (z -direction) compression of outer portions of the TPA. Conversely, the inner portion of the TPA wants to contract more or expand less than the TPA as a whole, and therefore these fibers would be in tension longitudinally. The precise location of this transition between tensile and compressive stresses through the cross section would depend on the result of elastic equilibrium resulting from the internal longitudinal stresses. We would expect that the balance of these forces would predict the experimental results shown in Fig. 6. The exact location of this transition may be the focus of future work, but we can nevertheless define an “inner” and “outer” region based on this location where we might expect a change from tensile to compressive thermally induced longitudinal stress.

In Fig. 6a, the model at most radii over-predicts untwist. For this amount of initial inserted twist the length change was best predicted by the inner most fibers (see Fig. 5a), suggesting that the majority of the TPA cross section would be considered in the “outer” region and in compression. In Fig. 6b, at the inner radii the model slightly over-predicts untwist while at the outer radii the model under-predicts untwist. For this amount of initial inserted twist the length change was well predicted by the fibers at $r = 0.5R$ (see Fig. 5b), and thus some fibers are “inner” and in tension while others are “outer” and in compression.

The radially varying longitudinal stress, σ_z , will lead to a shear stress when converting between axially aligned and polymer chain aligned coordinate systems. Using a proper transformation, this shear stress is $\tau_{12} = \sigma_z \sin \alpha \cos \alpha$. When the longitudinal stress is negative (compression), the fibers want to untwist more, and when the longitudinal stress is positive (tension), the fibers want to untwist less. As previously mentioned, we believe there is a larger region in compression for the less twisted TPA in Figs. 5a and 6a. For this reason, the experimental result show a large amount of untwist in Fig. 6a as compared to the model result at all radii. This is likely the result of compressive stresses resulting in significant shear deformation because of the lower α angles in the outer region.

Since these fibers are weak in shear, but stiff axially, it is expected that this shear stress will lead to a large shear strain. Figure 7 shows the axial and torsional modulus, E_1 and G_{12} , for

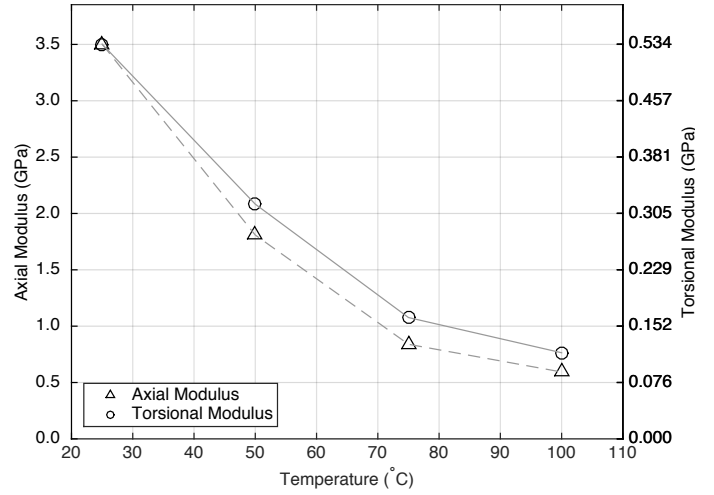


FIGURE 7: Experimental results for the axial modulus E_1 and torsional modulus G_{12} as a function of temperature.

the precursor fibers found experimentally from tension tests and torsion tests performed on the rheometer at various temperatures. Notice that G_{12} is approximately an order of magnitude less than E_1 . Based on this modulus, we would expect this shear stress to cause significant shear deformation, i.e. untwist of the outer fibers. Because this shear stress is due to the relationship between fibers at different radii, it is not captured by the current 2D model and the current models under-predicts untwist in the outermost fibers in Figs. 6a and 6b and over-predicts untwist in the inner fibers in Fig. 6b.

In the end, a 3D model may be necessary to capture some of the additional complexities from the interplay between fibers at different radii that are not captured by the current model. Or at a minimum, the 2D model will need to be revised to incorporate these internal stresses and express the change of length and untwist of the monofilament as a single entity which does not depend on radial position. One way to accomplish this would be to use the axial contraction as calculated from a balance of the longitudinal stresses to determine final TPA length wherein all layers are longitudinally coupled. Then, the same processes as used in this work could be used to calculate the untwist. These revised boundary conditions will introduce stresses into the material and so in addition to the thermal strains in Eq. (4)-(6), there will also be elastic strains, which will depend on the modulus parallel and perpendicular to the fibers, E_1 and E_2 , respectively, the shear modulus, G_{12} , and Poisson's ratio, ν_{12} . Determining these parameters presents significant experimental challenges, while deriving a revised 2D model or a 3D model will introduce significant more complexity to the model. Through this effort though, a model useful for design of these actuators will ensue.

5 Conclusions

This work presents a linear-elastic 2D model for twisted polymer actuators (TPAs) subject to thermal loading. The model is based on the assumption that the layers for TPAs at each radius are unaffected by adjacent layers at other radii, and thus the fibers are free to expand/contract and untwist due to thermal loading. Using this assumption, as well as classical kinematic relations for untwist and relationships between strain at different orientations, relations for thermal displacements are derived. Parameters for the model are identified on untwisted precursor fibers, so that minimal experimental tests are needed in the future for the design of TPAs. The resulting model is compared with experimental results from TPAs that were both fabricated and tested on a rheometer. In comparing experimental and modeling results, 3D effects appear to affect actuator performance and may be important to consider in future models of TPAs. The internal stresses that are expected across different radii would improve the predictions of untwist with the 2D model. Nonetheless, the 2D model at certain radii predict well the change in length and untwisting of the TPAs under thermal loading.

REFERENCES

- [1] Lima, M. D., Li, N., De Andrade, M. J., Fang, S., Oh, J., Spinks, G. M., Kozlov, M. E., Haines, C. S., Suh, D., Foroughi, J., et al., 2012. “Electrically, chemically, and photonically powered torsional and tensile actuation of hybrid carbon nanotube yarn muscles”. *Science*, **338**(6109), pp. 928–932.
- [2] Foroughi, J., Spinks, G. M., Wallace, G. G., Oh, J., Kozlov, M. E., Fang, S., Mirfakhrai, T., Madden, J. D., Shin, M. K., Kim, S. J., et al., 2011. “Torsional carbon nanotube artificial muscles”. *Science*, **334**(6055), pp. 494–497.
- [3] Haines, C. S., Lima, M. D., Li, N., Spinks, G. M., Foroughi, J., Madden, J. D., Kim, S. H., Fang, S., de Andrade, M. J., Göktepe, F., et al., 2014. “Artificial muscles from fishing line and sewing thread”. *Science*, **343**(6173), pp. 868–872.
- [4] Mirvakili, S. M., Ravandi, A. R., Hunter, I. W., Haines, C. S., Li, N., Foroughi, J., Naficy, S., Spinks, G. M., Baughman, R. H., and Madden, J. D., 2014. “Simple and strong: Twisted silver painted nylon artificial muscle actuated by joule heating”. In *SPIE Smart Structures and Materials+ Nondestructive Evaluation and Health Monitoring*, International Society for Optics and Photonics, pp. 90560I–90560I.
- [5] Cherubini, A., Moretti, G., Vertechy, R., and Fontana, M., 2015. “Experimental characterization of thermally-activated artificial muscles based on coiled nylon fishing lines”. *AIP Advances*, **5**(6), p. 067158.
- [6] Moretti, G., Cherubini, A., Vertechy, R., and Fontana, M., 2015. “Experimental characterization of a new class of polymeric-wire coiled transducers.”. In *SPIE Smart Structures and Materials+ Nondestructive Evaluation and Health Monitoring*, International Society for Optics and Photonics, pp. 94320P–94320P.
- [7] Aziz, S., Naficy, S., Foroughi, J., Brown, H. R., and Spinks, G. M., 2016. “Controlled and scalable torsional actuation of twisted nylon 6 fiber”. *Journal of Polymer Science Part B: Polymer Physics*, **54**(13), pp. 1278–1286.